Available online at www.sciencedirect.com
ScienceDirect
International Journal of Heat and Mass Transfer 51 (2008) 1431–1438
International Journal of HEAT and MASS TRANSFER
www.elsevier.com/locate/ijhmt

Effect of aggregation and interfacial thermal resistance on thermal conductivity of nanocomposites and colloidal nanofluids

William Evans [a,b], Ravi Prasher [c], Jacob Fish [b], Paul Meakin [d], Patrick Phelan [e], Pawel Keblinski [f,*]

[a] Lockheed Martin Corporation, 2401 River Road, Niskayuna, NY 12301, USA
[b] Mechanical Engineering Department, Rensselaer Polytechnic Institute, Troy, NY 12180, USA
[c] Intel Corporation, 5000 W. Chandler Blvd, Chandler, AZ 85226, USA
[d] Idaho National Laboratory, Center for Advanced Modeling and Simulation, P.O. Box 1625, Mail Stop 2211, Idaho Falls, ID 83415, USA
[e] Department of Mechanical and Aerospace Engineering, Arizona State University, Tempe, AZ 85287, USA
[f] Materials Science and Engineering Department, Rensselaer Polytechnic Institute, Troy, NY 12180, USA

Received 16 March 2007; received in revised form 10 September 2007
Available online 31 December 2007

Abstract

We analyzed the role of aggregation and interfacial thermal resistance on the effective thermal conductivity of nanofluids and nanocomposites. We found that the thermal conductivity of nanofluids and nanocomposites can be significantly enhanced by the aggregation of nanoparticles into clusters. The value of the thermal conductivity enhancement is determined by the cluster morphology, filler conductivity and interfacial thermal resistance. We also compared thermal conductivity enhancement due to aggregation with that associated with high-aspect ratio fillers, including fibers and plates.

Keywords: Nanoparticles; Aggregation; Thermal conductivity; Interfacial thermal resistance; Homogenization model; Monte Carlo simulation

1. Introduction

Understanding the mechanism and magnitude of enhanced thermal conductivity (k_{eff}) of nanoscale colloidal solutions (nanofluids) continues to be an active research area [1–3]. Understanding the mechanism was made particularly difficult by limited experimental characterization of the nanofluid, beyond thermal transport measurement. However, recently reported experimental studies [4–8] strongly support a notion that nanoparticle aggregation plays a significant role in thermal transport. In particular, Hong et al. [7] demonstrated by light scattering that Fe nanoparticles aggregate into micron size clusters leading to large conductivity increases. Kwak and Kim [8] demonstrated that large thermal conductivity enhancements are accompanied by sharp viscosity increases at low (<1%) nanoparticle volume fractions, which is indicative of aggregation effects. Lee et al. [6] demonstrated the critical importance of particle surface charge in nanofluid thermal conductivity. The surface charge is one of the primary factors controlling nanoparticle aggregation. Furthermore, Putnam et al. [9] and Zhang et al. [10] and Venerus et al. [11] demonstrated that nanofluids exhibiting good dispersion do not show any unusual enhancement of thermal conductivity.

Similarly to nanofluids, the desire to increase the thermal conductivity of thermally insulating materials is one of the motivations for incorporation of conductive fillers to solid, e.g., polymeric matrix. Nano/micro particle laden polymers are currently being used as thermal inter-

* Corresponding author. Present address: Department of Materials Science and Engineering, Rensselaer Polytechnic Institute, MRC 1st Floor, 110 8th Street, Troy, NY 12180, USA. Tel.: +1 518 2766858; fax: +1 518 2768554.
E-mail address: keblip@rpi.edu (P. Keblinski).

0017-9310/$ - see front matter © 2007 Elsevier Ltd. All rights reserved.
doi:10.1016/j.ijheatmasstransfer.2007.10.017

Nomenclature

A	area
A_k	Kapitza radius
a	radius of primary nanoparticles
D	diffusivity
d_l	chemical dimension
d_f	fractal dimension
dT/dZ	temperature gradient
f	volume fraction
k	thermal conductivity
N	number of particles
q	heat flux
$\mathbf{r}$	position vector
R_g	radius of gyration
T	temperature
t	time

Greek symbols

φ	volume fraction
τ	time

Subscripts

a	aggregate
c	backbone
eff	effective
f	fluid
l	liquid
nc	dead ends
p	particle

face materials and high conductivity mold compounds in electronics cooling [12,13]. Increasing the thermal conductivity of polymers using highly conducting particles is, therefore, very important. In both cases, solid composites and nanofluids, the key factors affecting thermal conductivity are the filler shape and dispersion/aggregation state. In the case of nanometer size fillers, another key parameter effecting thermal transport is the thermal interfacial resistance, also known as the Kapitza resistance R_k, which poses an additional barrier to the heat flow. In fact it is believed that the interfacial thermal resistance is the key factor limiting thermal performance in carbon nanotube composites and suspensions [14–16].

In this paper we present predictions of the three-level homogenization model that we recently introduced [17] on the effective thermal conductivity of nanofluids and nanocomposites. We will systematically evaluate the role of particle volume fraction, aggregation, conductivity, shape and the interfacial thermal resistance of the effective thermal conductivity. In particular, our treatment allows the effect of cluster morphology to be evaluated in terms of the average radius of gyration, R_g, of the aggregates and the fractal and chemical dimensions of the aggregates (d_f and d_l, respectively). We demonstrate that aggregates can lead to thermal conductivity enhancement that can be significantly higher than that predicted using homogenization theories of well dispersed composites. The thermal conductivity enhancement is mainly attributed to the ability of heat to move rapidly along the backbone of the cluster. Results of the homogenization model are validated by comparison with Monte Carlo (MC) numerical simulations of thermal conductivity of aggregate fractal structures prepared by a diffusion-limited cluster–cluster aggregation (DLCCA) algorithm. Finally, we compare results for the fractal aggregates to results obtained for high-aspect ratio inclusions including fibers and plates.

2. Homogenization model

Following well-established understanding of the fractal morphology of nanoparticle clusters in colloids [18], we built our three-level homogenization analysis based on the model depicted in Fig. 1. In accordance with Fig. 1, a fractal cluster is embedded within a sphere of radius equal to R_g and is composed of a few approximately linear chains, which span the whole cluster (aggregate) and side chains. The linear chains which span the whole cluster are called the backbone. The other particles, which do not span the whole cluster, are called dead ends [18]. The backbone plays a significant role in the rheology of colloids because it is the only structure that can transfer elastic forces between clusters [18]. Due to its connectivity, the backbone is also expected to play a crucial role in thermal conductivity.

Following the definition of the fractal dimension d_f, the number of particles in the cluster is given [19] by $N_{int} = (R_g/a)^{d_f}$, where a is the radius of the primary nano-

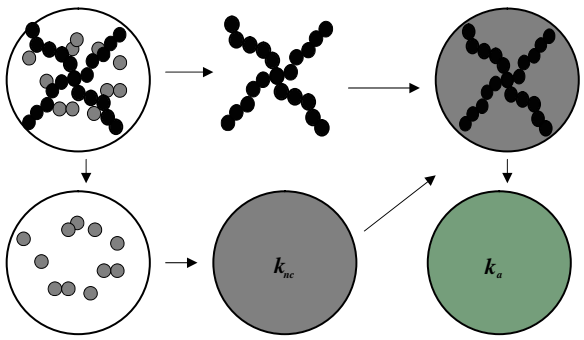

Fig. 1. Schematic of a single aggregate consisting of the backbone (black circles) and dead ends (gray circles). The aggregate is decomposed into dead ends with the fluid and the backbone. Thermal conductivity of the aggregate with only particles belonging to the dead ends, k_{nc}, is calculated using the Bruggeman model. In our homogenization model the linear chains are embedded inside a medium with effective conductivity of k_{nc}.

particle. Due to number conservation of the particles, $\phi_p = \phi_{int}\phi_a$, where ϕ_p is the volume fraction of the nanoparticles, ϕ_{int} is the volume fraction of the nanoparticles in the aggregate or the cluster, and ϕ_a is the volume fraction of the aggregates. It can be shown [19] that $\phi_{int} = (R_g/a)^{d_f-3}$ and [11] $(R_g/a)_{max} = (\phi_p)^{1/(d_f-3)}$ for which $\phi_a = 1$. The number of particles belonging to backbone, N_c, is defined by the chemical dimension, d_l, and is given [18] by $N_c = (R_g/a)^{d_l}$. d_l ranges between one and d_f. When $d_l = d_f$, all of the particles belong to the backbone and there are no dead ends. Therefore, the volume fraction of backbone particles (ϕ_c) in the aggregate is given by $\phi_c = (R_g/a)^{d_l-3}$. The volume fraction of the particles belonging to dead ends, ϕ_{nc}, is given by $\phi_{nc} = \phi_{int} - \phi_c$.

In the thermal model, the first level of homogenization is performed with only the particles belonging to the dead ends as shown in Fig. 1. The thermal conductivity of the aggregate due to dead end particles is calculated using the Bruggeman model, which is preferable when high volume fractions of highly conductive particles are involved. This model is given by [19]

$$(1-\phi_{nc})(k_l - k_{nc})/(k_l + 2k_{nc}) + \phi_{nc}(k_p - k_{nc})/(k_l + 2k_{nc}) = 0, \quad (1)$$

where k_{nc} is the effective thermal conductivity of the aggregate sphere in the presence of the dead-end particles only, k_p is the thermal conductivity of the nanoparticle, and k_l is the thermal conductivity of the liquid.

The effective thermal conductivity of the aggregate including the particles belonging to the backbone is calculated by assuming that the backbone is embedded in a medium with an effective conductivity of k_{nc}. Since the aspect ratio of the chains is significantly larger than one, we use the model by Nan et al. [20] for randomly oriented cylindrical particles. Using Nan's model, the effective thermal conductivity of the aggregate sphere, k_a, with both the chains and dead ends (Fig. 1) is given by

$$k_a = k_{nc}\frac{3 + \phi_c[2\beta_{11}(1-L_{11}) + \beta_{33}(1-L_{33})]}{3 - \phi_c[2\beta_{11}L_{11} + \beta_{33}L_{33}]}, \quad (2)$$

where

$$L_{11} = 0.5p^2/(p^2-1) - 0.5p\cosh^{-1}p/(p^2-1)^{1.5}, \quad (3)$$

$$L_{33} = 1 - 2L_{11} \quad \text{and} \quad (4)$$

$$\beta_{ii} = (k_{ii}^c - k_{nc})/[k_{nc} + L_{ii}(k_{ii}^c - k_{nc})]; \quad i = 1, 3. \quad (5)$$

p is the aspect ratio, which for the cluster spanning chain is given by $p = R_g/a$. Interfacial resistance is accounted for in the term

$$k_{ii}^c = k_p/(1.0 + \gamma L_{ii}k_p/k_l), \quad (6)$$

where $\gamma = (2 + 1/p)\alpha$ and $\alpha = A_k/a$. A_k is the Kapitza radius and represent a thickness of the matrix over which the temperature drop in a planar geometry, is the same as at the interface.

Finally, following Prasher et al. [19] and Wang et al. [4] the effective thermal conductivity of the whole system is calculated using the Maxwell–Garnet (M–G) model, where the volume fraction and the thermal conductivity of the aggregates are used. Therefore, the effective thermal conductivity of the whole system is given [12] by

$$k_{eff}/k_l = ([k_a + 2k_l] + 2\phi_a[k_a - k_l])/([k_a + 2k_l] - \phi_a[k_a - k_l]). \quad (7)$$

3. Monte Carlo simulations of model aggregates

3.1. Cluster generation

To provide a test bed for the homogenization procedure described above and to faithfully represent the well-known fractal nature of clusters observed in many colloidal suspensions of nanoparticles, we determined the thermal conductivity of model fractal aggregates obtained by diffusion controlled cluster–cluster aggregation. Cluster–cluster aggregation algorithms have been described in detail in the past [21]. In brief, we randomly marked 10,000 sites on a cubic lattice as filled to represent the nanoparticles. The remaining empty sites on the cubic lattice represent the volume occupied by the fluid. The overall size of the lattice was varied such that structures with particle volume fractions of 0.5%, 1.0%, 2.0%, and 4.0% were generated. For example, to represent the lowest volume fraction a lattice of size 126^3 was prepared. Starting from the initial structures, particles were allowed to diffuse and form clusters upon contact followed by cluster diffusion and cluster aggregation (see Fig. 2(a)). In our model, the cluster mobility is inversely proportional to the size of the cluster.

For each volume fraction, we prepared several independent sets of aggregates at various aggregation states ranging from approximately 9000 clusters (essentially no clustering) to a single large cluster. We characterized the aggregates by the average radius of gyration, R_g, where the average is weighted by the number of particles in each aggregate. As described extensively in the literature [21], such a cluster–cluster aggregation algorithm leads to fractal structures with $d_f \approx 1.8$ and $d_l \approx 1.4$. These values match the experimental data on diffusion controlled cluster aggregation well [18,21,22].

3.2. Effective thermal conductivity

The effective thermal conductivity of model fractal aggregate composites was obtained using a random walker Monte Carlo (MC) algorithm [23]. The MC simulations are performed on the same cubic lattice on which the aggregates are defined. Empty grid cells representing the liquid matrix are assigned a thermal conductivity, k_l. Cells occupied by the aggregate were assigned a thermal conductivity of k_p. The relative thermal conductivity increase is only

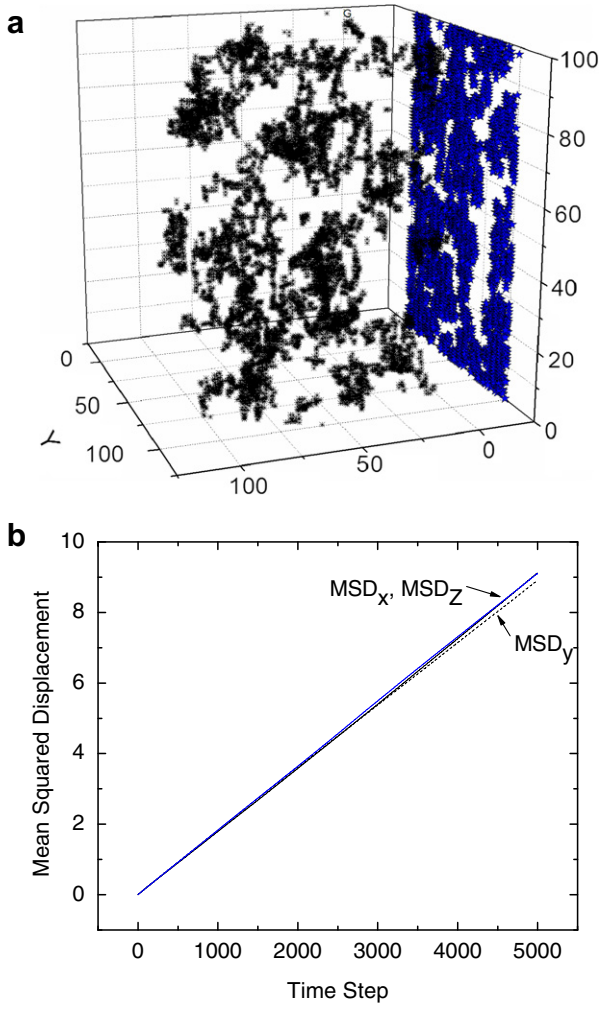

Fig. 2. (a) An aggregate structure obtained from the diffusion limited aggregation algorithm with 30 aggregates at 1% volume fraction. (b) A typical plot of the random walker's mean squared displacement over the simulation time (x, y and z components). The Einstein relation can then be used to obtain the diffusion coefficient which is proportional to thermal conductivity.

dependent on the ratio k_p/k_l. In our simulations, ratios from 50 to 400 were explored.

The MC simulation starts a random walker at a randomly chosen location on the cubic lattice. Then, the walker attempts to move randomly into one of the six directions on the cubic lattice. The probability of accepting the move, P, is calculated as $P = k_{in}/(k_{in} + k_{fi})$, where k_{in} and k_{fi} are the thermal conductivities of the cubes at which the walker resides and to which it attempts to move, respectively. The clock is advanced by the time proportional to $1/k_{in}$ regardless of the success of the move. The position of the random walker is continuously recorded for post processing which requires computation of the mean squared displacement. Each MC simulation involved about 0.5×10^6 MC steps, which is sufficient for adequate statistical accuracy.

The effective thermal conductivity of the aggregate system is proportional to the random walker diffusivity that can be evaluated using the well-known Einstein relation [24]

$$D = \lim_{\tau \to \infty} \frac{1}{6\tau} \langle |r(t+\tau) - \mathbf{r}(t)|^2 \rangle, \tag{8}$$

where the triangle brackets indicate average over multiple time origins, t, and $\mathbf{r}$ is the position vector of the random walker. In practice, the diffusivity is obtained from the mean squared displacement (MSD) vs. time slope. A typical simulation result is shown in Fig. 2(b). All reported diffusivities are normalized by the diffusivity of the pure matrix, which in turn gives the ratio of the composite/nanofluid conductivity to the pure matrix conductivity.

To ensure that the MC results are well converged and indeed represent the correct solutions of the diffusive heat flow equation for a selected structure we evaluated thermal conductivity by a thermodynamic finite element method (FEM) model. The model structure consisting of fluid and aggregate cubes was transferred to appropriate elements in a FEM model. At 0.5% volume fraction, 2×10^6 elements were required in the FEM model. A uniform heat flux, q, was imposed on two opposite faces of the cubic model. Adiabatic boundary conditions were established on the other faces. Under steady-state conditions, k_{eff} was calculated from Fourier's law

$$k_{eff} = qA \Big/ \frac{dT}{dZ}, \tag{9}$$

where A is the cube face area, and the temperature gradient, dT/dZ, is computed by FEM. The MC simulation and FEM model showed excellent agreement (within 2%).

4. Results

4.1. Homogenization model validation

Fig. 3 shows the effective thermal conductivity as a function of the average radius of gyration of the aggregates obtained both from homogenization theory and from MC simulations. For homogenization theory, we used parameters matching those characterizing the model fractal aggregates including $d_l = 1.4$, $d_f = 1.8$, and $k_p/k_l = 100$ and zero interfacial thermal resistance. The result of the homogenization theory and MC simulations match very well with all volume fractions and across the whole range of the aggregate sizes (measured by the radius of gyration). These are indeed quite remarkable results showing that a simple three-level homogenization model is able to quantitatively predict the effective thermal conductivity. It is also important to note that the critical aspect of the model is the explicit incorporation of the backbone into the model. Without the backbone present, i.e. treating the cluster as a disperse particle object, the homogenization model predicted conductivity is much lower and does not match the results of the MC simulations.

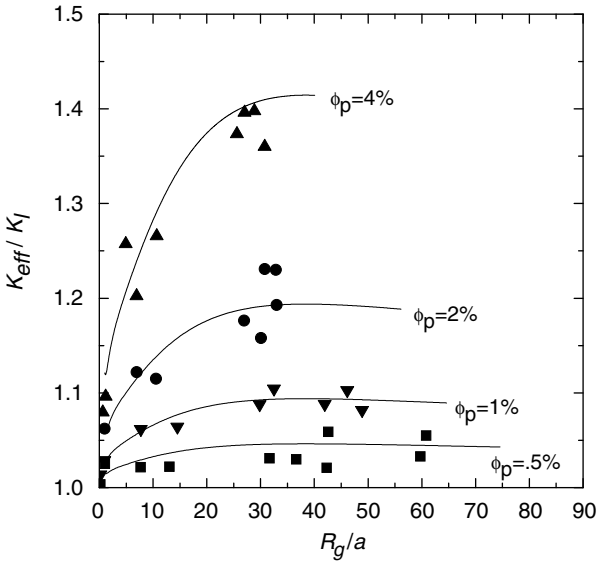

Fig. 3. Comparison between the three-level homogenization model (lines) and Monte Carlo simulation (symbols) for different values of particle volume fraction as a function of the radius of gyration illustrating good agreement between model and simulation. In all cases $k_p/k_l = 100$, $d_f = 1.8$ and $d_l = 1.4$.

4.2. Effect of the aggregation state

According to Fig. 3 the effective thermal conductivity increases rapidly with initial increase of the aggregate size and then saturates at the level dependent of the volume fraction. This increase is mainly caused by the increased size of the backbone that promotes rapid conduction across the cluster. Once, the clusters start to overlap, the conductivity reaches the maximum value that represent an interconnected network of nanoparticle clusters.

Since the backbone is primarily responsible for the thermal conductivity increases, one expects that bringing more particles to it, rather than to dead ends, will promote high thermal conduction. This is illustrated in Fig. 4 which shows the conductivity of fully aggregated structures at 0.5% volume fraction for structures with different chemical dimensions, d_l. The number of particles in the aggregate backbones increases with increasing chemical dimension, and for the chemical dimension equal to the fractal dimension all particles are in the backbone. As shown in Fig. 4, the latter case corresponds to maximum thermal conductivity. As a reference, the prediction of the effective medium theory for a fully dispersed composite shows much lower thermal conductivity increases than that of any structure with aggregated particles.

4.3. Effect of the particle conductivity

For well-dispersed spherical particles at low volume fractions the composite thermal conductivity is essentially particle conductivity independent, provided that the particle conductivity is about 10 times, or more, larger than the

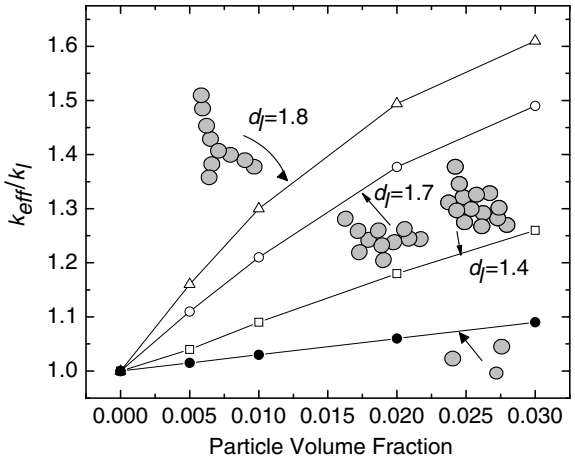

Fig. 4. Effect of chemical dimension on effective thermal conductivity for fully aggregated clusters ($k_p/k_l = 100$ at 0.5% volume fraction). As chemical dimension increases (1.4 squares, 1.7 circles, 1.8 triangles), an increasing number of particles join the backbone. For comparison purposes, effective medium theory results for fully dispersed particles are also shown.

matrix conductivity [25]. This is associated with the fact that particles act as constant temperature regions and the resistance to the heat flow comes only from the matrix. However, aggregation of the particles into clusters is expected to utilize the high particle conductivity more effectively.

Fig. 5 shows the effective thermal conductivity as a function of the average radius of gyration obtained both from homogenization theory and from the MC for 0.5% volume fraction for $k_p/k_l = 100$ and 200. Within the statistical fluctuations both models yield essentially the same results. Without aggregation ($R_g/a = 1$) the composite thermal conductivity predicted by the homogenization model is indeed independent from the particle conductivity. However, with increased aggregation the composite with

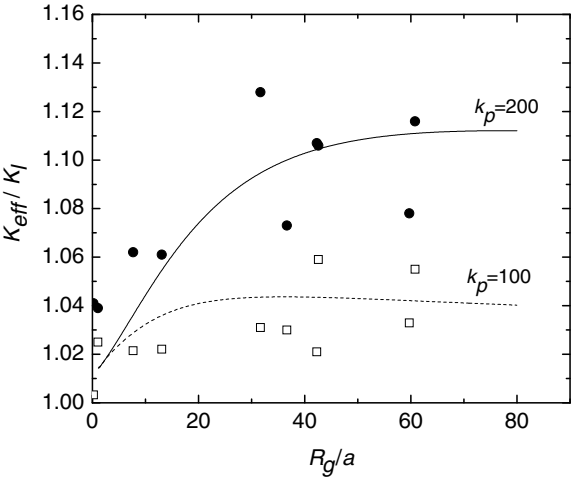

Fig. 5. The three-level homogenization model (lines) and Monte Carlo simulation results (symbols) for 0.5% volume fraction and $k_p/k_l = 200$ (solid lines and symbols) and $k_p/k_l = 100$ (dashed line and open symbols).

$k_p/k_l = 200$ consistently outperforms the one with $k_p/k_l = 100$ and for fully aggregated systems, $k_p/k_l = 200$ structure has thermal conductivity more than double that of $k_p/k_l = 100$ structure.

In Fig. 6 we compare the thermal conductivity of a fully aggregated systems i.e. for $(R_g/a)_{max} = (\phi_p)^{1/(d_f-3)}$ for values of k_p/k_l ranging from 25 to 200, and with chemical dimension equal to the fractal dimension (all particles in the backbone) to thermal conductivity of a composite consisting of randomly oriented cylinders. For randomly oriented long cylindrical objects for large k_p/k_l, k_{eff} varies as

$$\frac{k_{eff}}{k_l} = 1 + \varphi_p \frac{k_p}{3k_l}. \tag{10}$$

This represents an upper limit for conductivity enhancement within our model, which fully explores the high particle conductivity. Fig. 6 shows that at low volume fractions the conductivity characterizing composites of long cylinders matches very well with that obtained by the homogenization model. This is because in this region $(R_g/a)_{max}$ is large which makes the aspect ratio of the chain large. Finally, in Fig. 7 we show that thermal conductivity increase of the fully aggregated system at 0.5% volume fraction is proportional to k_p/k_l in perfect agreement with Eq. (10).

4.4. Effect of interfacial resistance

The interfacial resistance poses a barrier to heat flow that might inhibit the benefit of adding highly conductive filler. In this case, in the limit of low volume fractions of spherical, well-dispersed nanoparticles, all effective medium theories [25] predict

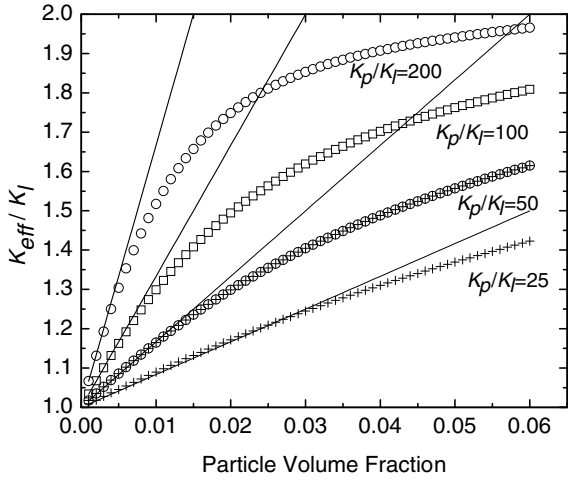

Fig. 6. Effective thermal conductivity of the nanofluid of a fully aggregated system (symbols) for different ratios of particle to fluid thermal conductivity. The lines are effective medium theory results for long cylinders as $k_p/k_l \to \infty$. In all cases, the fractal dimension is 1.8 and the chemical dimension is 1.4.

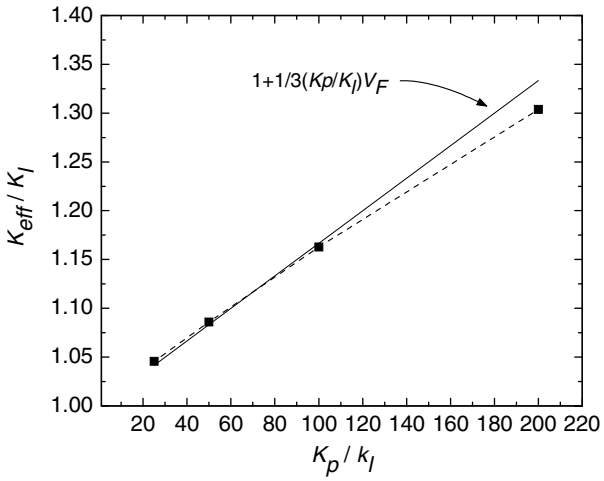

Fig. 7. The effect of the particle conductivity on fully aggregated system at 0.5% volume fraction, V_F, and the chemical dimension equal to the fractal dimension and equal 1.8. For comparison a solid line shows the prediction of the effective medium theory for randomly oriented long cylinders.

$$\frac{k_{eff}}{k_l} - 1 = 3f\frac{r/A_k - 1}{r/A_k + 2}, \tag{11}$$

where r is the particle radius and A_k is the Kapitza radius (see Section 2). According to Eq. (11) when the particle radius becomes equal to the Kapitza radius there is no enhancement at all, while for larger interfacial resistance the addition of particles decreases the thermal conductivity of the composite. From Eq. (11) it is clear that the interfacial resistance is more of a problem for small particles as for these particles the ratio r/A_k is small. A range of interfacial resistances reported for interfaces is from ~10 MW/m^2 K for weakly bonded (such as hydrophobic) interfaces [26] to ~100–300 MW/m^2 K for strongly bonded interfaces [27]. The corresponding Kapitza radius, assuming a low conductivity matrix, e.g. $k_f = 0.2$ W/m K, ranges from 20 nm to a fraction of nanometer. Therefore, for the majority of nanoparticles we expect that interfacial resistance will not significantly affect the composite conductivity. However, when small radius (or diameter) particles coincide with large interfacial resistance, such as is the case for single wall carbon nanotubes, the composite conductivity may be significantly diminished [15,20].

Interfacial resistance is accounted for in our 3-level homogenization model at level 1 for dead end particles and at level 2 for backbone particles. At level 2, interfacial resistance is incorporated in the Nan model as described in Section 2. For homogenization of the dead end particles at level 1, a particle of resistance $2a/k_p$ is considered to be in series with a Kapitza resistance $2R_b$ where the factor of 2 accounts for a resistance layer on each side of a slab (particle) of thickness $2a$. The equivalent combined resistance is then

$$\frac{2a}{k_{peff}} = \frac{2a}{k_p} + 2R_b. \tag{12}$$

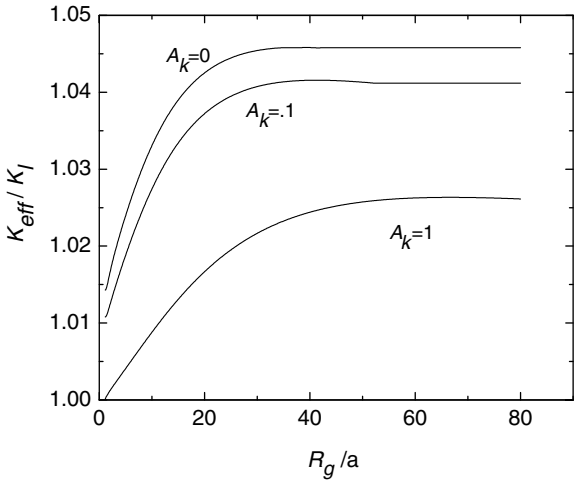

Fig. 8. Results of three-level homogenization theory with Kapitza interfacial resistance included for $k_p/k_l = 100$ at 0.5% volume fraction for various Kapitza radii.

The effective particle thermal conductivity, k_{peff}, is then

$$k_{peff} = \frac{k_p}{1 + \frac{R_b k_p}{a}}, \tag{13}$$

which replaces k_p in Eq. (1).

The role of the interfacial resistance for aggregated structures is demonstrated in Fig. 8. As expected, the interfacial resistance reduces the effective thermal conductivity of the composite. Without aggregation and with the Kapitza radius equal to the particle radius there is no thermal conductivity enhancement. However, with increasing cluster size much of the benefit of the high conductivity fillers is realized. For example, for $A_k = 1$, 0.5% particle volume fraction, and $k_p/k_l = 100$, k_{eff} increase is about 2.5% of the matrix conductivity vs. about 4% with the zero interfacial resistance.

5. Discussion

Our analysis and simulations demonstrates that aggregation of high conductive nanoparticles in a liquid or solid low-conductivity matrix contributes to significant thermal conductivity enhancement. The key underlying factor is the high aspect ratio backbone of the fractal-like aggregates that allows for rapid heat flow over large distances. The high aspect ratio is also capable of diminishing a negative role of interfacial thermal resistance on thermal transport. For cases where well dispersed composites show low thermal conductivity enhancement, composites with fractal aggregates show significant enhancements, even with substantial interfacial resistance.

The above observations, quite naturally, suggest in the design of the high-thermal conductivity materials that the key factor is the high-aspect ratio of the filler, coming either from sparse aggregates or particles with intrinsically high aspect ratio. To illustrate the effect of the particle shape, we compare our results for fractal aggregates (Fig. 8) with the effective medium results for fiber and flat plate nanoparticles composites calculated according to Nan et al. [20]. Fig. 9 shows k_{eff} for randomly oriented fibers and randomly oriented flat plates as a function of the aspect ratio. Both fibers and plates show greater enhancement in thermal conductivity than aggregates. The key reason is the fact that in the aggregates some particles are in dead ends and thus contribute little to thermal transport. As discussed before, if all particles are in the backbone the aggregates are as good as randomly dispersed fibers or plates.

Fig. 9 also shows the effect of increasing interfacial thermal resistance for fibers and plates. At fixed volume fraction and aspect ratio, the thermal conductivity enhancement decreases much more with increasing interfacial resistance for plates than for long fibers.

These results suggest that the optimum design for nanofluids and nanocomposites for thermal conductivity enhancement would involve the use of high-aspect-ratio fibers, e.g. single wall carbon nanotubes, rather than spherical or ellipsoidal particles. On the other hand, single wall carbon nanotubes are characterized by high interfacial thermal resistance with fluids and solids, which inhibits the potential of thermal conductivity increases [28]. Furthermore, long fibers tend to curl in the liquid of polymer matrix reducing the effective length of the fiber.

When synthesizing nanofluids and nanocomposites with spherical nanoparticles, the most effective heat conduction increases will be achieved with purposely chained nanoparticles with very few, if any, particles forming dead ends (that is, aggregates with large chemical dimension) since dead end particles provide little benefit to the thermal conductivity of the system. It is, however, important to notice that the use of large aggregates or high aspect ratio fillers in fluids will lead to dramatic increases in fluid viscosity [29]

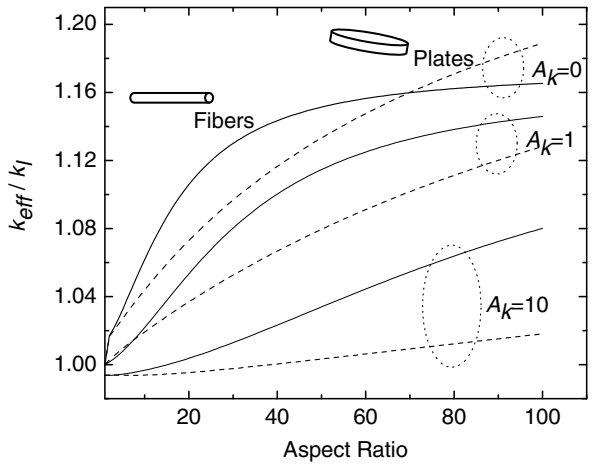

Fig. 9. Comparison of the effective medium theory predictions for randomly oriented long fibers (solid curves) and flat plates (dashed curves) for $k_p/k_l = 100$ at 0.5% volume fraction showing the effects of increasing interfacial resistance.

which might render this fluid useless in applications requiring fluid flow.

6. Conclusions

By using three-level homogenization theory, validated by MC simulation of heat conduction on model fractal aggregates, we have demonstrated based purely on thermal conduction physics that the thermal conductivity of nanofluids and nanocomposites can be significantly enhanced as a result of aggregation of the nanoparticles. The conductivity enhancement due to aggregation is also a strong function of the chemical dimension of the aggregates and the radius of gyration of the aggregates. The model developed in this paper accounts for aggregation kinetics and the impact of chemistry of the system through their dependence of the radius of gyration [19]. By including the effect of interfacial thermal resistance in the homogenization model, we have also shown that any enhancement in the thermal conductivity will be degraded; however, this degradation can be limited by large aggregate sizes.

References

[1] P. Keblinski, J.A. Eastman, D. Cahill, Nanofluids for thermal transport, Materials Today 8 (23) (2005) 36–44.
[2] R.S. Prasher, P. Bhattacharya, P.E. Phelan, Thermal conductivity of nanoscale colloidal solutions (nanofluids), Phys. Rev. Lett. 94 (2005) 025901-1–025901-4.
[3] W. Evans, J. Fish, P. Keblinski, Role of Brownian motion hydrodynamics on nanofluid thermal conductivity, Appl. Phy. Lett. 88 (2006) 093116-1–093116-3.
[4] B.-X. Wang, L.P. Zhou, X.F. Peng, A fractal model for predicting the effective thermal conductivity of liquid with suspension of nanoparticles, Int. J. Heat Mass Transfer 46 (14) (2003) 2665–2672.
[5] Y. Xuan, Q. Li, W. Hu, Aggregation structure and thermal conductivity of nanofluids, AIChE J. 49 (4) (2003) 1038–1043.
[6] D. Lee, J.W. Kim, B.G. Kim, A new parameter to control heat transport in nanofluids: surface charge state of the particle in suspension, J. Phys. Chem. B 110 (2006) 4323–4328.
[7] K.S. Hong, T.K. Hong, H.S. Yang, Thermal conductivity of Fe nanofluids depending on the cluster size of nanoparticles, Appl. Phy. Lett. 88 (2006) 031901-1–031901-3.
[8] K. Kwak, C. Kim, Viscosity and thermal conductivity of copper oxide nanofluid dispersed in ethylene glycol, Korea–Australia Rheol. J. 17 (35) (2005) 35–40.
[9] A. Putnam, D.G. Cahill, P.V. Braun, Z.B. Ge, R.G. Shimin, Thermal conductivity of nanoparticles suspensions, J. Appl. Phys. 99 (2006) 084308-1–084308-6.
[10] X. Zhang, H. Gu, M. Fujii, Experimental study on the effective thermal conductivity and thermal diffusivity of nanofluid, Int. J. Thermophys. 27 (2) (2006) 569–580.
[11] D.C. Venerus, M.S. Kabadi, S. Lee, V. Perez-Luna, Study of thermal transport in nanoparticle suspensions using forced Rayleigh scattering, J. Appl. Phys. 100 (2006) 094310-1–094310-2.
[12] R.S. Prasher, Thermal interface materials: historical perspective, status, and future directions, Proc. IEEE 94 (8) (2006) 1571–1586.
[13] R.S. Prasher, P. Koning, J. Shipley, S. Prstic, J.L. Wang, Thermal resistance of particle laden polymeric thermal interface materials, J. Heat Transfer 125 (6) (2003) 1170–1177.
[14] M.J. Biercuk, M.C. Llaguno, M. Radosavljevic, J.K. Hyun, A.T. Johnson, J.E. Fischer, Appl. Phys. Lett. 80 (15) (2002) 2767–2769.
[15] S.T. Huxtable, D.G. Cahill, S. Shenogin, L. Xue, R. Ozisik, P. Barone, M. Usrey, M.S. Strano, G. Siddons, M. Shim, P. Keblinski, Interfacial heat flow in carbon nanotube suspensions, Nat. Mater. 2 (2003) 731–734.
[16] S.U.S. Choi, Z.G. Zhang, W. Yu, F.E. Lockwood, E.A. Grulke, Anomalous thermal conductivity enhancement in nanotube suspensions, Appl. Phys. Lett. 79 (14) (2001) 2252–2254.
[17] R. Prasher, W. Evans, P. Meakin, J. Fish, P. Phelan, P. Keblinski, Effect of aggregation on thermal conduction in colloidal nanofluids, Appl. Phys. Lett. 89 (2006) 143119-1–143119-2.
[18] W.-H. Shih, W.Y. Shih, S.-I. Kim, J. Liu, I.A. Aksay, Scaling behavior of the elastic properties of colloidal gels, Phys. Rev. A 42 (1990) 4772–4779;
R. de Rooji, A.A. Potanin, D. van den Ende, J. Mellema, Steady shear viscosity of weakly aggregating polystyrene latex dispersions, J. Chem. Phys. 99 (11) (1993) 9213–9223.
[19] R. Prasher, P.E. Phelan, P. Bhattacharya, Effect of aggregation kinetics on the thermal conductivity of nanoscale colloidal solutions (nanofluid), Nano Lett. 6 (7) (2006) 1529–1534.
[20] Ce-Wen Nan, R. Birringer, D.R. Clarke, H. Gleiter, Effective thermal conductivity of particulate composites with interfacial thermal resistance, J. Appl. Phys. 81 (10) (1997) 6692–6699.
[21] P. Meakin, Formation of fractal clusters and networks by irreversible diffusion-limited aggregation, Phys. Rev. Lett. 51 (13) (1982) 1119–1122;
M. Kolb, R. Boter, R. Jullien, Scaling of kinetically growing clusters, Phys. Rev. Lett. 51 (13) (1983) 1119–1122;
P. Meakin, Fractal aggregates, Adv. Colloid Interf. Sci. 28 (4) (1988) 249–331;
P. Meakin, I. Majid, S. Havlin, H.E. Stanley, Topological properties of diffusion limited aggregation and cluster–cluster aggregation, J. Phys. A: Math. Gen. 17 (18) (1984) L975–L981.
[22] B. Russel, D.A. Saville, W.R. Schowalter, M.J. Ablowitz, S.H. Davis, E.J. Hinch, A. Iserles, J. Ockendon, P.J. Olver, Colloidal Dispersion, Cambridge University Press, Cambridge, 1992;
R.J. Hunter, Foundations of Colloid Science, Oxford University Press, New York, 1992.
[23] C.DeW. Van Siclen, Walker diffusion method for calculation of properties of composite materials, Phys. Rev. E 59 (3) (1999) 2804–2807.
[24] M.P. Allen, D.J. Tildesley, Computer Simulation of Liquids, Oxford University Press, Oxford, 2003.
[25] S.A. Putnam, D.G. Cahill, B.J. Ash, L.S. Schadler, High-precision thermal conductivity measurements as a probe of polymer/nanoparticles interfaces, J. Appl. Phys. 94 (10) (2003) 6785–6788.
[26] Z.B. Ge, D.G. Cahill, P.V. Braun, AuPd metal nanoparticles as probes of nanoscale thermal transport in aqueous solution, J. Phys. Chem. B 108 (49) (2004) 18870–18875.
[27] A. Plech, V. Kotaidis, S. Gresillon, C. Dahmen, G. von Plessen, Laser-induced heating and melting of gold nanoparticles studied by time-resolved X-ray scattering, Phys. Rev. B 70 (2004) 195423-1–195423-7.
[28] S. Shenogin, L. Xue, R. Ozisik, P. Keblinski, D.G. Cahill, Role of thermal boundary resistance on the heat flow in carbon-nanotube composites, J. Appl. Phys. 95 (12) (2004) 8136–8144.
[29] S.R. Raghavan, S.A. Khan, Shear-thickening response of fumed silica suspensions under steady and oscillatory shear, J. Colloid Interf. Sci. 185 (1997) 57–67.